Piercing Unit Geodesic Disks*

Ahmad Biniaz† Prosenjit Bose‡ Thomas Shermer§

Abstract

We prove that at most 3 points are always sufficient to pierce a set of m pairwise-intersecting unit geodesic disks inside a simple polygon P with n vertices of which n_r are reflex. We provide an $O(n + m \log n_r)$ time algorithm to compute these at most 3 piercing points. Our bound is tight since it is known that in certain cases 3 points are necessary.

1 Introduction

The study of problems related to piercing a collection of convex sets has a rich history in Computational Geometry [10]. One of the most famous results in this area is Helly's theorem [15, 16] which states the following: Given n convex sets in $\Re^d$, with $n > d$, if every $d + 1$ convex sets have a nonempty intersection, then all n sets have a nonempty intersection. In other words, if a point pierces every $d + 1$ sets, then a point pierces all n sets. For Helly's theorem to hold, it is critical that every $d+1$ sets have a point in common. Helly's theorem no longer holds if only d sets have a point in common. For example, given n lines in the plane, i.e. $d = 2$, where every pair of lines intersects but no three have a point in common, then $\Omega(n)$ points are required to pierce every line. On the other hand, given a set of n pairwise-intersecting disks in the plane, Danzer and Stachó independently showed that 4 points pierce all the disks [9, 22, 23]. Grünbaum [11] showed that 4 points are sometimes necessary thereby proving optimality. Neither the proof by Danzer nor the proof by Stachó lends itself to an efficient algorithm to actually compute these 4 points. From a computational perspective, Har-Peled et al. [14] presented a linear time algorithm to compute 5 points that pierce a set of pairwise-intersecting disks. Biniaz et al. [6] presented a simple linear time algorithm to find 5 piercing points using elementary geometric observations. Carmi et al. [8] presented a fairly involved linear time algorithm to compute 4 piercing points. In the case of a set of pairwise-intersecting unit disks, Hadwiger and Debrunner [13] showed that 3 points are sufficient to pierce the set. Biniaz et al. [6] showed that 3 points are sometimes necessary and presented a simple linear time algorithm to compute the piercing points. It is the fact that disks are *fat*, as opposed to lines which are *thin*, that allows a constant number of points to pierce pairwise-intersecting disks. This relationship between the number of points needed to pierce a family of planar pairwise-intersecting convex sets and the *fatness* of these sets has been explored in the literature [2, 5, 18, 20]. The most recent result we know of is by Bazarghani et al. [5] who show that $O(\alpha)$ points can pierce a set of pairwise-intersecting α-fat convex sets. Although there are several definitions of *fatness* in the literature, the definition that is used in [5] is the following: a convex set C is deemed α-fat if the ratio of the radius of the smallest disk that contains C and the largest disk that is contained in C is at most α.

In this paper, we focus on piercing problems in the geodesic setting. Specifically, we explore the following question: given a set of pairwise-intersecting geodesic disks inside a simple polygon, can a constant number of points pierce every disk? Given a simple polygon P, a geodesic disk centered on a point $x \in P$ is the set of points $y \in P$ such that the length of the shortest path from x to y in P is at most a constant r, the radius. This setting is more general than the setting in the Euclidean plane. In this setting, Bose et al. [7] showed that 14 points suffice to pierce a set of pairwise-intersecting geodesic disks inside a simple polygon and gave an $O(n+m \log n_r)$ time algorithm to compute these at most 14 piercing points where n is the number of vertices of P, n_r is the number of reflex vertices and m is the number of geodesic disks. Subsequently, Abu-Affash et al. [1] showed that 5 points suffice in this setting and provide an $O((n+m) \log n_r)$ time algorithm to find these 5 piercing points. This upper bound may not be tight, since the best known lower bound on the number of points required to pierce a set of pairwise-intersecting geodesic disks is 4. Our main result is the following: we show that 3 points are always sufficient to pierce a set of pairwise-intersecting unit geodesic disks inside a simple polygon and provide an $O(n + m \log n_r)$ time algorithm to compute these 3 piercing points. Our bound is tight since the lower bound of 3 points in the plane also holds in the more general geodesic setting.

*Research support in part by NSERC.

†School of Computer Science, University of Windsor, abiniaz@uwindsor.ca

‡School of Computer Science, Carleton University, jit@scs.carleton.ca

§School of Computing Science, Simon Fraser University, shermer@sfu.ca

2 Notation and Preliminaries

Before presenting our main results, we first introduce some notation and preliminary lemmas. Let $P = v_0, \ldots, v_{n-1}$ be a simple n-vertex polygon. We use the convention that the interior of P lies to the right of the edge directed from v_i to v_{i+1}, i.e. the polygon is described in a clockwise fashion. In what follows, index manipulation is modulo the size of the set. In the case of the polygon, it is modulo n.

A segment between two points a, b is denoted as ab and its length is denoted as $|ab|$. Given two points $x, y \in P$, the geodesic (or shortest) path from x to y in P is denoted $\Pi(x, y)$. The length of this path, referred to as the *geodesic distance*, is the sum of the lengths of its edges and is denoted by $|\Pi(x, y)|$. The *geodesic metric* refers to P together with the geodesic distance function. A subset S of P is *geodesically convex* if, for all pairs of points $x, y \in S$, the geodesic path in P between x and y (i.e. $\Pi(x, y)$) is in S. Pollack et al. [21] proved the following lemma about distances between a point and a geodesic path.

Lemma 1 *[21] Let a, b, c be 3 distinct points in P. Define the function $g : \Pi(b, c) \rightarrow \Re$, as $g(x) = |\Pi(a, x)|$. Then g is a convex function with its maximum occurring either at b or c.*

Informally, a polygon P is *weakly simple* provided that a slight perturbation of the points on the boundary results in a simple polygon. See Akitaya et al. [4] for a formal definition of weakly-simple polygons as well as an algorithm to quickly recognize such polygons. A *pseudo-triangle* is a simple polygon with 3 convex vertices (the shaded region in Figure 1 is a pseudo-triangle). A *geodesic triangle* on points $a, b, c \in P$, denoted $\triangle(a, b, c)$, is a weakly-simple polygon whose boundary consists of $\Pi(a, b), \Pi(b, c)$ and $\Pi(c, a)$. In Figure 1, $\triangle(c_0, c_1, c_2)$ consists of the red paths and the shaded region. A *geodesic hexagon* is defined in a similar fashion but on six points in P. Let $X = \{x_0, x_1, \ldots, x_k\}$ be a set of at least 3 points in P. The set X is *geodesically collinear* if $\exists x_i, x_j \in X$ such that $X \subset \Pi(x_i, x_j)$. Given points a, b, and c in P that are not geodesically collinear, the shortest paths $\Pi(a, b)$ and $\Pi(a, c)$ follow a common path from a until they diverge at a point a' (note that a' could be a). Similarly, let b' be the point where $\Pi(b, a)$ and $\Pi(b, c)$ diverge, and c' be the point where $\Pi(c, a)$ and $\Pi(c, b)$ diverge. The geodesic triangle $\triangle(a', b', c')$ is simple (not weakly simple), has a', b', and c' as its convex vertices, and is a pseudo-triangle. We refer to $\triangle(a', b', c')$ as the *geodesic core* of $\triangle(a, b, c)$ and denote it as $\nabla(a, b, c)$; the shaded region in Figure 1 is the geodesic core of $\triangle(c_0, c_1, c_2)$. These properties were also observed in Pollack et al. [21].

This leads to a natural generalization of the notions of orientation, angles, and sidedness for geodesics. Given two distinct points $a, b \in P$, the *orientation* of a point a with respect to b in P is the counter-clockwise angle that the first edge of $\Pi(a, b)$ makes with the positive x-axis. Orientations are between 0 (inclusive) and 2π (exclusive). Given 3 points $a, b, c \in P$ that are not geodesically collinear, we denote by $\angle abc$ the convex angle at b' in the geodesic core $\nabla(a, b, c)$. When a, b, c are geodesically collinear then $\angle abc$ is π if $b \in \Pi(a, c)$, and 0 otherwise. We say that b is to the left of $\Pi(a, c)$ if the convex vertices in $\nabla(a, b, c)$ appear in the order a', b', c' when traversing the boundary in clockwise order starting at a'; otherwise, b is to the right. When referring to points of P to the left or right of an edge ab of P, we consider ab to be $\Pi(a, b)$.

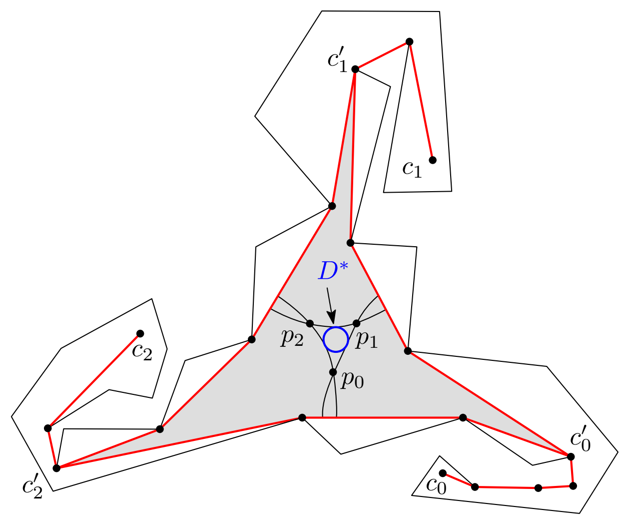

Figure 1: Basic definitions.

A *geodesic disk* centered at $c \in P$ with radius $r \geq 0$ is the set $\{y \in P : |\Pi(c, y)| \leq r\}$. A geodesic disk is geodesically convex and its boundary may be composed of several arcs of different curvature [21]. Two geodesic disks are *tangent* when the geodesic distance between the centers of the disks is exactly the sum of the radii. A *unit* geodesic disk is a geodesic disk with radius 1.

3 Upper bound on number of piercing points

In this section, we prove that 3 points suffice to pierce any set of pairwise-intersecting geodesic unit disks. Throughout this paper, we will be working with a collection $\mathcal{D} = \{D_0, D_1, \ldots, D_{m-1}\}$ of pairwise-intersecting unit geodesic disks whose respective centers $c_0, c_1, \ldots c_{m-1}$ are in P. We define D^* as the smallest geodesic disk that intersects each member of $\mathcal{D}$, with c^* and r^* being the center and radius of D^*, respectively. The set $\mathcal{D}$ is called *Helly* if there is one point that pierces all the disks. Every disk in $\mathcal{D}$, by definition, intersects D^*. We use D^* to compute the 3 points that suffice to pierce $\mathcal{D}$, when $\mathcal{D}$ is not Helly. The following lemma about properties of D^* when $\mathcal{D}$ is not Helly, proven in [7], will be useful in the sequel.

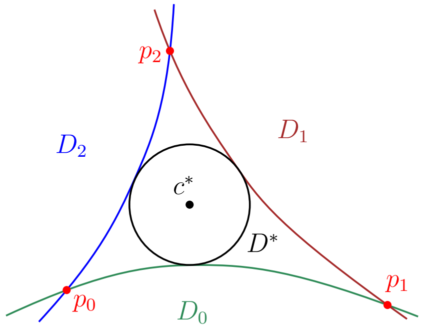

Figure 2: Close-up of p_0, p_1, p_2.

Lemma 2 *[7] If $\mathcal{D}$ is* **not** *Helly, then the disk D^* has the following properties:*

1. *the radius $r^* > 0$, where r^* is the radius of D^*,*
2. *D^* is tangent to at least 3 geodesic disks D_0, D_1, D_2 in $\mathcal{D}$ at 3 distinct points t_0, t_1 and t_2, respectively,*
3. *D^* does not intersect the boundary of the geodesic core $\nabla(c_0, c_1, c_2)$, where c_i is the center of disk D_i, for $i \in \{0, 1, 2\}$,*
4. *The boundary of D^* is a circle,*
5. *c^* is contained in the interior of $\triangle(t_0, t_1, t_2)$.*

The properties of D^* that are important to note are the following. First, even though D^* is a geodesic disk in P, its boundary is actually a circle that does not intersect the boundary of P; see Figure 1. Second, the fact that $\mathcal{D}$ consists of pairwise-intersecting unit disks implies that D^* must be tangent to 3 disks in $\mathcal{D}$ as opposed to 2, which can be the case when the disks are not pairwise-intersecting. In the remainder of the paper, we use the notation in Lemma 2 to refer to the three disks tangent to D^*, their tangency points, and centers. We begin by giving an upper bound on the radius r^* of D^*.

Lemma 3 *The radius r^* of D^* is at most $(2/\sqrt{3}) - 1$.*

Proof. If $\mathcal{D}$ is Helly, then $r^* = 0$, thus, we only need to consider the case when $\mathcal{D}$ is not Helly. Since $\sum_{i=0}^{2} \angle c_i c^* c_{i+1} = 2\pi$, we can assume without loss of generality that $\angle c_1 c^* c_2 \geq 2\pi/3$. Denote by ray$(a, b)$ the half-line with initial point a containing b. Let c^*b_1 be the first edge of $\Pi(c^*, c_1)$, as in Figure 4. Define b'_1 as the first point along ray(c^*, b_1) where it intersects with $\Pi(c_1, c_2)$. This intersection must exist by the Jordan Curve Theorem [24] since c^* is inside $\nabla(c_0 c_1 c_2)$. Note that it may be the case that b'_1 is b_1. Let c'_1 be the point on ray(c^*, b'_1) such that $|c^*c'_1| = |\Pi(c^*, c_1)|$. Define b'_2 and c'_2 analogously. The segment $c^*c'_1$ can be viewed as an *unfolding* of $\Pi(c^*, c_1)$ onto ray(c^*, b'_1). Thus, since D^* and D_1 are tangent, we have that $|\Pi(c^*, c_1)| = |c^*c'_1| = |c^*b'_1| + |b'_1c'_1| = 1 + r^*$. Similarly, $|\Pi(c^*, c_2)| = |c^*b'_2| + |b'_2c'_2| = 1 + r^*$. Since $\angle c'_1 c^* c'_2 \geq 2\pi/3$, by the cosine law, we have that $|c'_1c'_2| \geq \sqrt{3}(1 + r^*)$.

By the triangle inequality of the geodesic metric, $|\Pi(c^*, c_1)| \leq |c^*b'_1| + |\Pi(b'_1, c_1)|$. Since $|\Pi(c^*, c_1)| = |c^*b'_1| + |b'_1c'_1|$, we have that $|b'_1c'_1| \leq |\Pi(b'_1, c_1)|$. By the same argument, $|b'_2c'_2| \leq |\Pi(b'_2, c_2)|$. Therefore, we have that $|\Pi(c_1, c_2)| = |\Pi(c_1, b'_1)| + |\Pi(b'_1, b'_2)| + |\Pi(b'_2, c_2)| \geq |c'_1b'_1| + |\Pi(b'_1, b'_2)| + |b'_2c'_2| \geq |c'_1c'_2|$.

Since D_1 and D_2 have unit radius and intersect, we have that $2 \geq |\Pi(c_1, c_2)| \geq |c'_1c'_2| \geq \sqrt{3}(1 + r^*)$. We conclude that $r^* \leq (2/\sqrt{3}) - 1$.

□

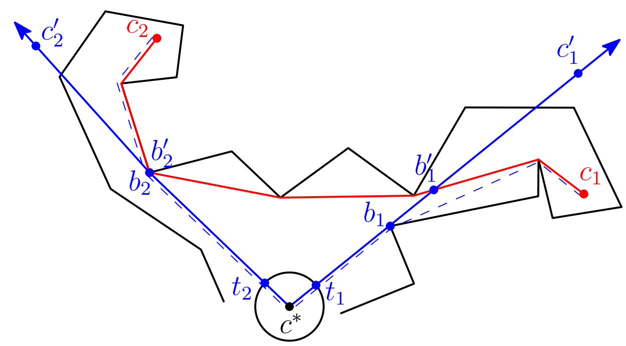

Figure 4: Illustration of the proof of Lemma 3.

For $i \in \{0, 1, 2\}$, let p_i be the point of $D_i \cap D_{i-1}$ closest to c^* (Figure 2). These points must exist because the disks in $\mathcal{D}$ are pairwise-intersecting. Moreover, in our main theorem, we will prove that these three points pierce the set $\mathcal{D}$.

Lemma 4 *The points p_0, p_1 and p_2 are in the geodesic core $\nabla(c_0, c_1, c_2)$.*

Proof. We show that $p_2 \in \nabla(c_0, c_1, c_2)$. The same argument shows that both p_1 and p_0 are in $\nabla(c_0, c_1, c_2)$. Consider $\triangle(b'_1, b'_2, c^*)$ where b'_1 and b'_2 are defined as in the proof of Lemma 3 and illustrated in Figure 4. Recall that $|\Pi(c^*, c_1)| = 1 + r^*$ since D_1 is tangent to D^*. By construction, we have that $|\Pi(c^*, c_1)| = |c^*b'_1| + |b'_1c'_1|$. Since $|c^*b'_1| > r^*$, we have that $|b'_1c'_1| = |\Pi(c_1, b'_1)| < 1$. Note that by construction of b'_1, we have that $\Pi(c_1, c_2) = \Pi(c_1, b'_1) + \Pi(b'_1, c_2)$. Given that $|\Pi(c_1, b'_1)| < 1$, we have that the boundary of D_1 intersects $\Pi(c_1, c_2)$ at a point x on $\Pi(b'_1, c_2)$. Similarly, the boundary of D_2 intersects $\Pi(c_1, c_2)$ at a point y on $\Pi(b'_2, c_1)$.

By construction, we have that c^* is a convex vertex of the geodesic triangle $\triangle(b'_1, b'_2, c^*)$. Since D_1 and D_2

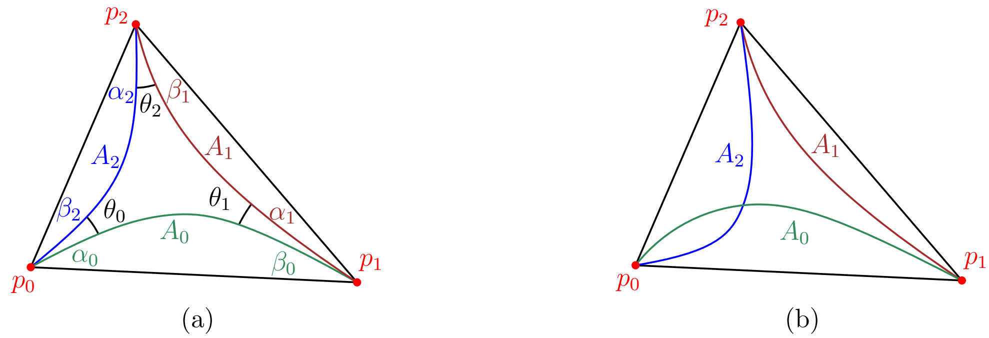

Figure 3: Points, arcs, and angles.

intersect, we have that $|\Pi(c_1, c_2)| \leq 2$. If $|\Pi(c_1, c_2)| = 2$, in other words, the point x and y coincide, then p_2 is on $\Pi(c_1, c_2)$ and therefore $p_2 \in \nabla(c_0, c_1, c_2)$. Otherwise, we consider the case when $|\Pi(c_1, c_2)| < 2$. In this case, notice that as we traverse $\Pi(c_1, c_2)$ from c_1 to c_2, we must encounter y before x.

Consider the arc B_1 to be the portion of the boundary of D_1 from t_1, the point of tangency between D_1 and D^*, to x. Since this arc at t_1 enters $\triangle(b'_1, b'_2, c^*)$, by the Jordan curve theorem [24], it intersects either $\Pi(b'_1, b'_2)$ or the segment $c^*b'_2$. Let us consider the latter case first. Assume that B_1 intersects $c^*b'_2$ at a point z. Let B'_1 be the portion of B_1 from t_1 to z. Consider the closed region R consisting of the segment zc^*, the segment c^*t_1 and B'_1. We now define the arc B_2 to be the portion of the boundary of D_2 from t_2 to y. At t_2, the arc B_2 enters the region R. Since y is outside of R, by the Jordan curve theorem, B_2 must intersect the boundary of R. This intersection point, which is p_2, must be on B'_1 since B_2 cannot intersect c^*t_1 as every point on that segment is farther than 1 from c_2. Thus, p_2 is in $\triangle(b'_1, b'_2, c^*)$ since B'_1 is.

For the case where B_1 intersects $\Pi(b'_1, b'_2)$, we use the same argument except that the boundary of the region R consists of B_1, $\Pi(x, b'_2)$, b'_2c^* and c^*t_1. Since we encounter y before x when we traverse $\Pi(c_1, c_2)$ from c_1 to c_2, the point y is outside R. Thus B_2 must intersect the boundary of R, and similar to previous case this intersection which is p_2 must be through B_1 in the triangle $\triangle(b'_1, b'_2, c^*)$. Therefore, we have that $p_2 \in \nabla(c_0, c_1, c_2)$. □

By the proof of Lemma 4, p_2 lies in $\triangle(b'_1, b'_2, c^*)$ which is essentially a star shaped polygon with center c^*. Thus the segment c^*p_2 lies in $\triangle(b'_1, b'_2, c^*)$ which is a subset of $\nabla(c_0, c_1, c_2)$. Applying a similar argument to p_0 and p_1 we have the following corollaries.

Corollary 5 *The line segment c^*p_i is in $\nabla(c_0, c_1, c_2)$.*

Recall c'_0, c'_1, and c'_2 as the convex vertices of the geodesic core $\nabla(c_0, c_1, c_2)$.

Corollary 6 *The geodesic hexagon $c'_0p_1c'_1p_2c'_2p_0$ is a subset of the geodesic triangle $\triangle c_0c_1c_2$.*

Refer to Figure 3(a) for the following. For $i \in \{0, 1, 2\}$, let A_i be the arc on the boundary of D_i from p_i to p_{i+1}. Let θ_i be the clockwise angle from A_{i-1} to A_i at p_i. If $\theta_i = 0$ then the disks D_{i-1} and D_i are tangent at p_i. If $\theta_i > 0$ then D_{i-1} and D_i have a positive area of overlap, starting at p_i. The case when $\theta_i < 0$ cannot happen since p_i is the intersection point closest to c^*. Note this in Figure 3(b) where p_0 should be at the other intersection of arcs A_0 and A_2.

For $i \in \{0, 1, 2\}$, let α_i be the angle from A_i to the line segment p_ip_{i+1} at p_i, and β_i be the angle from A_i to the line segment p_ip_{i+1} at p_{i+1}; see Figure 3(a).

Lemma 7 *For $i \in \{0, 1, 2\}$, $|p_ip_{i+1}| \leq 1$.*

Proof. Consider a parameter s that denotes the distance we have moved as we move from p_i to p_{i+1} along A_i. The coordinates of a point $x \in A_i$ as well as the tangent t to A_i at point x can be expressed as a function of this parameter s. See Figure 5, where the tangents are shown as red arrows. Let Δt denote the change in angle of this tangent from p_i to p_{i+1}. Then $\Delta t = \alpha_i + \beta_i$. This can be seen in the figure, letting q be the point where the tangent is parallel to the segment p_ip_{i+1}. Then the tangent sweeps out α_i as it moves from p_i to q, and then sweeps out β_i as it moves from q to p_i.

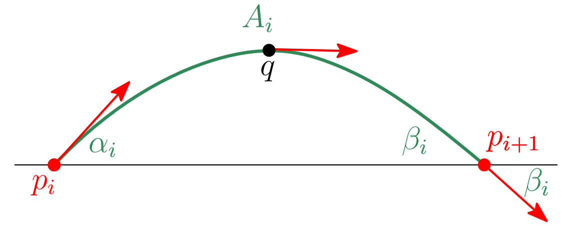

Figure 5: Tangents to A_i.

Let $\kappa(s)$ denote the curvature of A_i with respect to parameter s. Then, by definition of the integral of curvature taken along A_i, we have that $\Delta t = \int_{A_i} \kappa(s)ds$.

Since D_i is a unit geodesic disk, it has curvature at least 1 on all of its boundary arcs. This is because every boundary arc of D_i comes from a circle whose radius is at most 1. Since $\kappa(s) \geq 1$, we have $\Delta t \geq \int_{A_i} 1 ds$. But the latter integral is simply the length of the arc A_i. Since $\alpha_i + \beta_i = \Delta t$, we have that $\alpha_i + \beta_i \geq |A_i|$.

Because of the lower bound of 1 on the curvature, the length of A_i will be at least as large as the length of a (uniformly) curvature-1 curve from p_i to p_{i+1} This uniform curve is a circular arc A'_i of radius 1 with some center which we denote as c'_i; see Figure 6. Denote by C'_i the unit circle centered at c'_i. We have $A'_i \subset C'_i$.

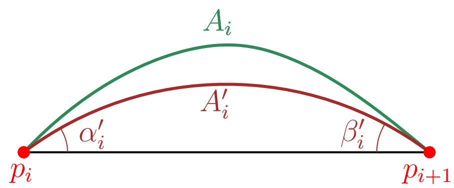

Figure 6: A curvature-1 curve A'_i.

Claim 1 *For $i \in \{0,1,2\}, |p_i p_{i+1}|$ is maximized when C'_0, C'_1, and C'_2 are pairwise tangent.*

Proof. By definition, C'_i and C'_{i+1} have a non-empty intersection. Define L'_i as the line through c'_i and c'_{i+1}. For sake of a contradiction, we first consider the case where none of the disks are tangent to each other but $|p_i p_{i+1}|$ is maximized. Move c'_0 in the direction perpendicular to L'_1 away from L'_1 until C'_0 becomes tangent to either C'_1 or C'_2. During this process, p_2 remains fixed and p_0p_2, p_1p_2, p_0p_1 increase in length, which is a contradiction. Now, without loss of generality, assume that only C'_0 and C'_1 are tangent. By moving c'_2 in the direction perpendicular to L'_0 away from L'_0 until C'_2 becomes tangent to either C'_0 or C'_1, once again, p_1 remained fixed and p_0p_1, p_1p_2, p_0p_2 increase in length, which is a contradiction. Finally, without loss of generality, assume that only C'_0 and C'_2 are not tangent. Rotate C'_0 around c'_1, while keeping it tangent to C'_1, until C'_0 is tangent to C'_2. Here we note that p_2 remains fixed, and p_0p_2, p_1p_2, p_0p_1 increase in length. Therefore, we conclude that each $|p_i p_{i+1}|$ is maximized when C'_0, C'_1, and C'_2 are pairwise tangent. This finishes our proof of Claim 1.

By Claim 1, each $|p_i p_{i+1}|$ is maximized when C'_0, C'_1, and C'_2 are pairwise tangent, in which case $\triangle(p_0, p_1, p_2)$ must be an equilateral triangle with side length 1. □

Corollary 8 *For $i \in \{0, 1, 2\}$,*

$$|c^* p_i| \leq \sqrt{r^*(2 + r^*)} \leq 0.578.$$

Proof. Using the same transformation as in the proof of Claim 1, we can see that for $i \in \{0, 1, 2\}$, $|c^* p_i|$ is maximized when the circles C'_i are pairwise tangent and the points p_0, p_1, p_2 form an equilateral triangle. This means that c'_i, c^* and p_i form a right triangle with side lengths $1, 1 + r^*$ and $|c^* p_i|$. Pythagoras' theorem gives the bound on $|c^* p_i|$ and the numerical upper bound we get from the upper bound on r^* in Lemma 3. □

Theorem 9 *Let $\mathcal{D}$ be a collection of pairwise-intersecting unit geodesic disks inside a simple polygon P. Then there are three points inside P such that each disk of $\mathcal{D}$ contains at least one of the points.*

Proof. Let D^+ be the radius-$1 + r^*$ geodesic disk centered at c^*, and C^+ be the geodesic circle that is the boundary of D^+. The circle C^+ contains arcs at distance $1 + r^*$ from c^* and segments of the boundary of P at distances less than that. If we extend the line segment $c^* p_i$ in a straight line from p_i, we will hit C^+ at some point q_i (which could be the same as p_i). The c_i's (the centers of the three disks tangent to D^*) and q_i's divide the circle C^+ into six sections; we concentrate on the section between c_1 and q_1; a symmetric argument applies to the other five sections.

Since both ends of $\Pi(c_1, c_0)$ are at geodesic distance $1 + r^*$ from c^*, any point on $\Pi(c_1, c_0)$ is at distance no more than $1 + r^*$ from c^* (by Lemma 1). This implies that the arcs of C^+ (which are at distance $1+r^*$ from c^*) do not intersect the interior of the geodesic core of the geodesic triangle $\triangle c_0c_1c_2$. Since there is no boundary of P in the interior of any geodesic core, the segments of C^+ also do not intersect the interior of the geodesic core of $\triangle c_0c_1c_2$. Because this is true for all six sections of C^+, C^+ does not intersect the interior of the geodesic core.

Let c_T be a point on C^+ non-strictly between c_1 and q_1. Because c_T is not in the interior of the geodesic core of $\triangle c_0c_1c_2$, $\Pi(c_T, c^*)$ intersects $\Pi(c_1, c_0)$. This implies that $\Pi(c_T, c^*)$ also intersects $\Pi(c_1, p1)$, as the geodesic hexagon $c'_0p_1c'_1p_2c'_2p_0$ (which contains c^*) must be inside the geodesic core of $\triangle c_0c_1c_2$, by Corollary 6. Let u be the intersection point of $\Pi(c_T, c^*)$ and $\Pi(c_1, p1)$, and let t_T be the point where $\Pi(c_T, c^*)$ crosses the boundary of D^*. See Figure 7.

The distance $d(c_1, p_1)$ is equal to $d(c_1, u) + d(u, p_1) = 1$ since p_1 is on the boundary of D_1. The distance $d(c_1, u) + d(u, t_T) \geq 1$, since D_1 is tangent to D^*. So $d(u, t_T) \geq d(u, p_1)$ and therefore $d(c_T, u) + d(u, t_T) \geq d(c_T, u) + d(u, p_1)$. The left-hand side of that last inequality is simply 1, and the right-hand side is an upper bound on the distance $d(c_T, p_1)$, so we get $1 \geq d(c_T, p_1)$, or that p_1 pierces the disk of radius one centered at c_T.

Now consider a unit disk D in our collection of disks $\mathcal{D}$. The center c of D lies inside the radius $1 + r^*$ disk around c^*, and without loss of generality, it lies in a

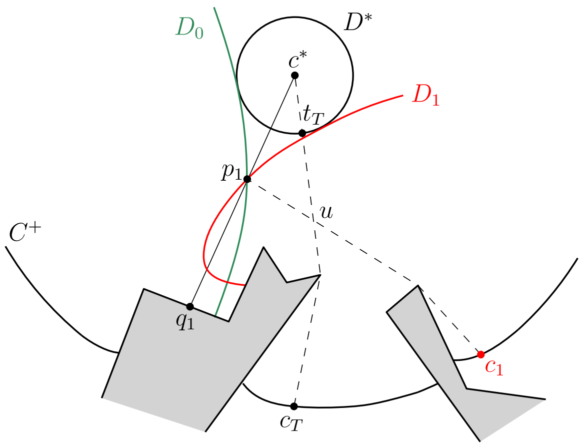

Figure 7: $\Pi(c_T, c^*)$ intersects $\Pi(c_1, p_1)$ at u.

direction between c_1 and p_1 from c^*. We extend the last segment of $\Pi(c^*, c)$ until it reaches the radius $1+r^*$ circle at a point c_T. The center c lies on $\Pi(c_T, c^*)$, the distance $d(c_T, p_1) \leq 1$ as discussed above, and the distance $d(c^*, p_1) \leq 1$ (by Corollary 8). Thus $d(c, p_1) \leq 1$ by Lemma 1, and hence p_1 pierces D.

Therefore, the three points p_0, p_1, and p_2 pierce the entire collection $\mathcal{D}$. □

4 Algorithmic Considerations

In this section, we describe an algorithm to compute the piercing points. The input to the algorithm is $\mathcal{D}$. First, compute D^* in $O(n+m \log n_r)$ time using the algorithm described in [7]. This is achieved since it was shown in [7] that computing D^* is an LP-type problem.

The reason that the run-time has a $\log n_r$ term as opposed to a $\log n$ term is that given a polygon P, we first apply a geodesic-preserving simplification of P in $O(n)$ time to get a polygon $P' \supset P$ of size $O(n_r)$ where n_r is the number of reflex vertices in P, such that the shortest path from x to y in P is identical to the shortest path from x to y in P' [3]. Then, we preprocess P' in $O(n_r)$ time to answer in $O(\log n_r)$ time the length of the shortest path from x to y and $O(\log n_r + k)$ to report the k edges on the shortest path [12, 17]. With these tools in hand, Bose et al. [7] apply Matousek et al.'s [19] general framework for solving LP-type problems to find D^* within the stated amount of time.

If $r^* = 0$, then c^* is returned as the point that pierces $\mathcal{D}$. If $r^* > 0$, then in $O(n)$ time, compute $\nabla(c_0c_1c_2)$ with 3 queries to the shortest path data structure constructed above. Now all that remains is to compute p_0, p_1 and p_2. We show how to compute p_0 in $O(n)$ time. The other two points are computed in a similar manner. Recall t_i as the point of tangency between D^* and D_i. To compute p_0, we need to intersect the arc A_0 with the arc A_2. Each arc A_i consists of at most n_r pieces of circular arcs inside $\nabla(c_0c_1c_2)$. Essentially, to find p_0, we walk along A_0 from t_0 towards $\Pi(c_0, c_2)$, and along A_2 from t_2 towards $\Pi(c_0, c_2)$. By always advancing on the arc that is furthest away from $\Pi(c_0, c_2)$, we eventually find p_0 in $O(n)$ time.

The cost of finding p_0, p_1, p_2 is dominated by the cost of finding D^*. We conclude with the following:

Theorem 10 *Given a set $\mathcal{D}$ of m pairwise-intersecting disks in a simple polygon P on n vertices and n_r reflex vertices, we can compute the at most 3 points that pierce $\mathcal{D}$ in $O(n + m \log n_r)$ time.*

5 Conclusion

Theorem 10 settles the question of how many points are sufficient to pierce a set of pairwise-intersecting unit disks in the geodesic setting. It would be interesting to prove that the runtime of our algorithm is optimal. We leave as an open question to determine whether 4 or 5 points are necessary to pierce pairwise-intersecting geodesic disks of arbitrary radius. When the radii are arbitrary, 4 points are sometimes necessary and always sufficient in the Euclidean setting. In the geodesic setting, the best known lower bound is 4 (from the lower bound example in the Euclidean setting) and the upper bound is 5 piercing points [1]. It would be interesting to close this gap.

References

[1] A. K. Abu-Affash, P. Carmi, and M. Maman. Piercing pairwise intersecting geodesic disks by five points. *Comput. Geom.*, 109:101947, 2023.

[2] P. K. Agarwal, M. J. Katz, and M. Sharir. Computing depth orders for fat objects and related problems. *Computational Geometry: Theory and Applications*, 5(4):187–206, 1995.

[3] O. Aichholzer, T. Hackl, M. Korman, A. Pilz, and B. Vogtenhuber. Geodesic-preserving polygon simplification. *Int. J. Comput. Geometry Appl.*, 24(4):307–324, 2014.

[4] H. A. Akitaya, G. Aloupis, J. Erickson, and C. D. Tóth. Recognizing weakly simple polygons. *Discret. Comput. Geom.*, 58(4):785–821, 2017.

[5] S. Bazargani, A. Biniaz, and P. Bose. Piercing pairwise intersecting convex shapes in the plane. In *LATIN*, volume 13568 of *Lecture Notes in Computer Science*, pages 679–695. Springer, 2022.

[6] A. Biniaz, P. Bose, and Y. Wang. Simple linear time algorithms for piercing pairwise intersecting disks. In *CCCG*, pages 228–236, 2021 (to appear in CGTA).

[7] P. Bose, P. Carmi, and T. C. Shermer. Piercing pairwise intersecting geodesic disks. *Comput. Geom.*, 98:101774, 2021.

[8] P. Carmi, M. J. Katz, and P. Morin. Stabbing pairwise intersecting disks by four points. *CoRR*, abs/1812.06907, 2018.

[9] L. Danzer. Zur Lösung des Gallaischen Problems über Kreisscheiben in der Euklidischen Ebene. *Studia Scientiarum Mathematicarum Hungarica*, 21(1-2):111–134, 1986.

[10] J. E. Goodman, J. O'Rourke, and C. Toth, editors. *Handbook of Discrete and Computational Geometry, Third Edition*. Chapman and Hall/CRC, 2017.

[11] B. Grünbaum. On intersections of similar sets. *Portugal. Math.*, 18:155–164, 1959.

[12] L. J. Guibas and J. Hershberger. Optimal shortest path queries in a simple polygon. *J. Comput. Syst. Sci.*, 39(2):126–152, 1989.

[13] H. Hadwiger and H. Debrunner. Ausgewählte Einzelprobleme der kombinatorischen Geometrie in der Ebene. *Enseignement Math. (2)*, 1:56–89, 1955.

[14] S. Har-Peled, H. Kaplan, W. Mulzer, L. Roditty, P. Seiferth, M. Sharir, and M. Willert. Stabbing pairwise intersecting disks by five points. *Discret. Math.*, 344(7):112403, 2021.

[15] E. Helly. Über Mengen konvexer Körper mit gemeinschaftlichen Punkten. *Jahresbericht der Deutschen Mathematiker-Vereinigung*, 32:175–176, 1923.

[16] E. Helly. Über Systeme von abgeschlossenen Mengen mit gemeinschaftlichen Punkten. *Monatshefte für Mathematik*, 37(1):281–302, 1930.

[17] J. Hershberger. A new data structure for shortest path queries in a simple polygon. *Inf. Process. Lett.*, 38(5):231–235, 1991.

[18] M. J. Katz. 3-d vertical ray shooting and 2-d point enclosure, range searching, and arc shooting amidst convex fat objects. *Computational Geometry*, 8(6):299–316, 1997.

[19] J. Matousek, M. Sharir, and E. Welzl. A subexponential bound for linear programming. *Algorithmica*, 16(4/5):498–516, 1996.

[20] F. Nielsen. On point covers of c-oriented polygons. *Theo. Comp. Sci.*, 265(1–2):17–29, 2001.

[21] R. Pollack, M. Sharir, and G. Rote. Computing the geodesic center of a simple polygon. *Discrete & Computational Geometry*, 4:611–626, 1989.

[22] L. Stachó. Über ein Problem für Kreisscheibenfamilien. *Acta Scientiarum Mathematicarum (Szeged)*, 26:273–282, 1965.

[23] L. Stachó. A gallai-féle körletuzési probléma megoldása. *Mat. Lapok*, 32(1-3):19–47, 1981-84.

[24] C. Thomassen. The jordan–schönflies theorem and the classification of surfaces. *American Mathematical Monthly*, 99(2):116–130, 1992.